Influence of C, Mn and Ni Contents on Microstructure and Properties of Strong Steel Weld Metals — Part III. Increased Strength from Carbon Additions

E. Keehan*, L. Karlsson**, H.-O. Andrén* and H. K. D. H. Bhadeshia***

* Department of Experimental Physics, Chalmers University
of Technology, SE – 412 96 Gothenburg, Sweden

** ESAB AB, P.O. Box 8004, SE – 402 77 Gothenburg, Sweden.

***University of Cambridge, Department of Materials Science and
Metallurgy, Pembroke Street, Cambridge CB2 3QZ, U.K.

Abstract

Neural network predictions suggested that strength of a high strength steel weld metal with 7 wt. % nickel and 0.5 wt. % manganese could be increased significantly at moderate expense to impact toughness by additions of carbon. Based on this, three experimental weld metals were produced with carbon levels between 0.03 and 0.11 wt. %. Mechanical test results were in agreement with predictions. With low carbon content the microstructure was largely bainitic in dendrite core regions while martensite was found at interdendritic regions. From microstructural studies and dilatometry experiments it was found that carbon stabilised austenite to lower transformation temperatures and that the microstructure became more martensitic in nature. Effects on strength and impact toughness were explainable in terms of a refinement of the microstructure and tempering behaviour.

Introduction

Welding research metallurgists have attempted to address the contradictory problems of higher strength, increased ductility and good weldability without sacrificing impact toughness for shield metal arc welding since the 1960's [1–3]. Following a trend of decreasing carbon concentration in high strength steel manufacture, the path of reducing carbon content was also pursued with carbon contents even lower than 0.01 wt. % tested [4]. Weld metals with such low carbon content are largely dependant on other alloying elements such as manganese, nickel, chromium and molybdenum for strength. They have good weldability and as alloying content or cooling rate is increased the microstructure becomes mainly that of bainite and martensite.

Recently, neural network modelling has been used as a development tool in many aspects of materials science. The advantages this technique offers are described elsewhere [5–7]. Using the composition of a commercial shielded metal arc welding (SMAW) electrode (ESAB OK 75.78; 3Ni, 2Mn, 0.5Cr, 0.6Mo, 0.05C wt. %) as a starting point, it was predicted using neural network modelling that nickel must be added in a controlled manner with respect to manganese at a carbon content of 0.03 wt. %, otherwise impact toughness is greatly reduced [8]. These predictions were confirmed experimentally and found to be in agreement with literature where similar compositions were studied [4, 9]. It was concluded from this work that the optimum alloying content of these elements was 0.5 wt. % manganese and 7 wt. % nickel in order to achieve both high strength and good impact toughness [8]. High resolution microstructural studies methods found the microstructure to be mainly that of upper bainite, lower bainite and a previously unreported constituent in weld metals described as coalesced bainite along with some martensite [10–12].

Manganese and nickel were set at their optimum values of 0.5 and 7.0 wt. %, respectively, and the modelling was continued further for other alloying elements. It was predicted that strength could be increased at moderate expense to impact toughness by carbon additions as shown in Figures 1 and 2 [13]. Three experimental weld metals were produced with carbon contents at 0.03, 0.06 and 0.11 wt. %. This is the third paper in a series of three that investigate the effects of variations in alloying content of nickel, manganese and carbon in high strength steel weld metals. The paper focuses on carbon presenting results from high resolution microstructural investigations where the fine scale microstructure is characterised and links are made with the mechanical properties.
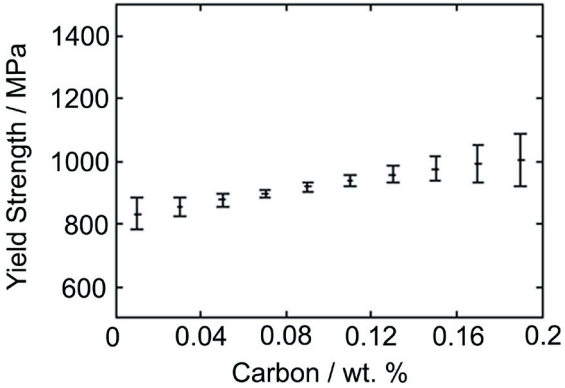
Figure 1 Predicted yield strength as a function of carbon concentration for the base composition 0.034 C, 0.25 Si, 0.5 Cr and 0.62 Mo. The error bars represent ± 1 σ of uncertainty [13].
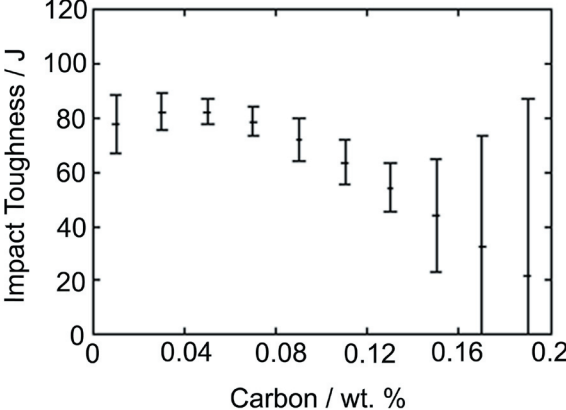
Figure 2 Predicted impact toughness at –60 ºC as a function of carbon concentration for the base composition given in the caption of Figure 1. The error bars represent ± 1 σ of uncertainty [13].

Experimental Procedures

The welded joints were made as described previously [11]. The welding parameters and chemical compositions are presented in Table 1. Weld metals were named 7-0.5L200, 7-0.5M200 and 7-0.5H200 where 7 is the nickel content, 0.5 is the manganese content, L, M, H stand for the carbon contents (low, medium and high) and 200 is the interpass temperature in °C.

Specimens for Charpy–V impact testing, tensile testing, dilatometry and metallographic analysis (light optical microscopy (LOM), field emission gun scanning electron microscopy (FEG-SEM), transmission electron microscopy (TEM)) were prepared as described elsewhere [11]. Once microstructural studies were complete, hardness measurements were carried out on cross sections using the Vickers method with a 10 kg load (HV10). In total 16 indents were made starting in the last bead proceeding down the centre of the welded joint in 1 mm steps.

	7-0.5L200	7-0.5M200	7-0.5H200
E / kJ mm^{-1}	1.3	1.4	1.3
IPT / °C	200	200	200
$t_{8/5}$ / s	10	11	10
C *	0.030	0.061	0.110
Mn	0.61	0.56	0.53
Ni	6.11	6.84	7.04
Cr	0.16	0.15	0.14
Si	0.4	0.34	0.38
S*	0.009	0.006	0.007
P	0.010	0.011	0.008
Mo	0.38	0.35	0.40
V	0.018	0.014	0.016
Cu	0.02	0.01	n.a.
O / ppm*	340	350	260
N / ppm*	150	160	100
YS / MPa	777	858	912
UTS / MPa	831	895	971
YS / UTS	0.94	0.96	0.94
A_5 / %	22	18	18

Table 1 Welding parameters, chemical composition and recorded tensile properties. Welding parameters presented are energy input (E), interpass temperature (I.P.T.) and the estimated cooling time between 800 and 500 °C ($t_{8/5}$) calculated from WeldCalc [14]. Composition is in wt. % unless otherwise stated, n.a. is not analysed and '*' indicate elements analysed using Leco Combustion equipment.

Results

Mechanical Properties

Tensile properties and Charpy impact toughness levels are presented in Table 1 and Figure 3. In short, it was confirmed that increasing carbon from 0.03 to 0.11 wt. % increased yield strength, going from 778 to 912 MPa. In spite of this large increase in strength, impact toughness remained high with 78 J at – 40 °C and 63 J at – 100 °C for the weld metal with 0.11 wt. %. C.

The results of hardness measurements are plotted in Figure 4. As was expected, hardness increased with increase in carbon content. The hardness of the last bead increased around 80 Vickers from approximately 320 to 400 Vickers as a result of changing carbon from 0.03 to 0.11 wt. %. On entering the central reheated regions a large decrease in hardness was experienced for all alloys with weld metal 7-0.5H200 most affected. Also in reheated regions the weld metals followed the trend of higher hardness with greater carbon content.
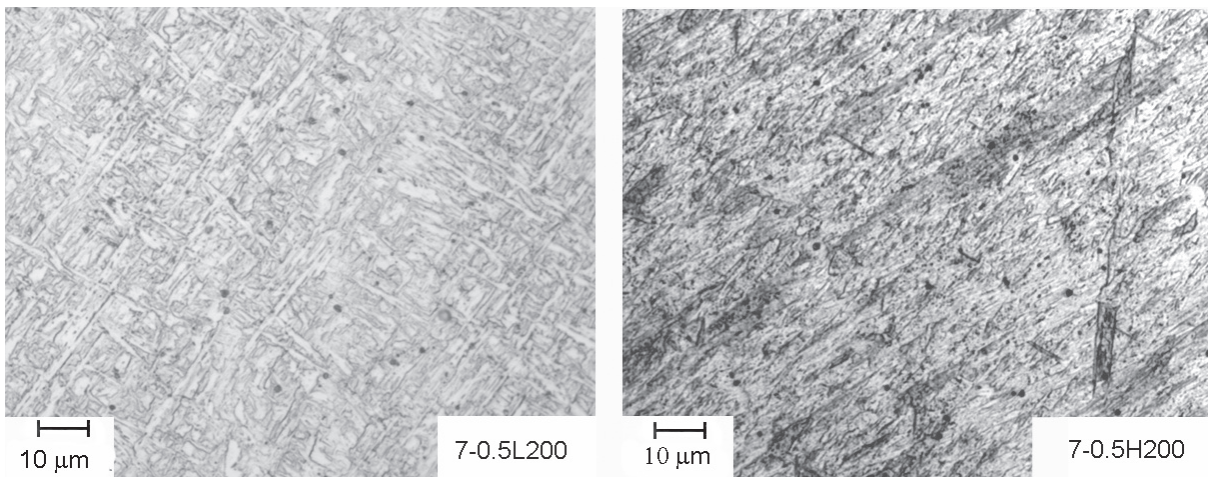
Microstructure — Last Bead

Optical micrographs showing a fine scale microstructure are presented in Figure 5. As is commonly found for high strength steel weld metals it was difficult to decipher whether the microstructure was martensite or bainite due to their similar morphologies [9, 15]. FEGSEM was therefore employed and proved to be a very revealing method. Investigations were carried out on all three samples with only selected results presented here for the high and low carbon weld metals.
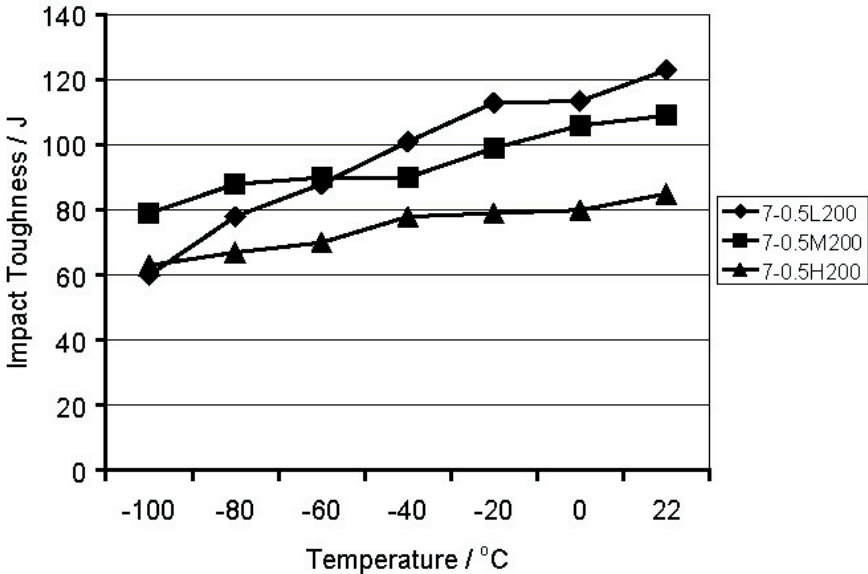
Figure 3 Charpy–V impact toughness plots illustrating the effect of increasing carbon from 0.03 to 0.11 wt. %
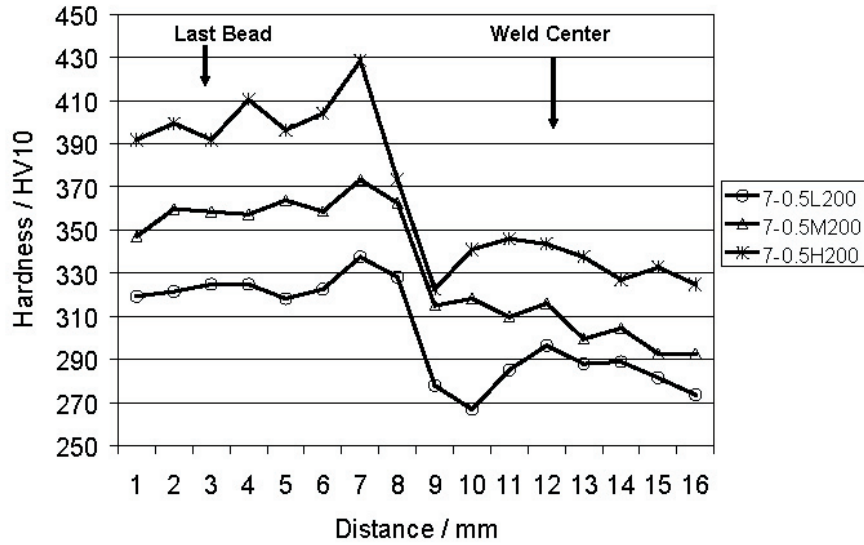
Figure 4 Hardness plots starting in the last bead showing the effect of increasing carbon from 0.03 to 0.11 wt. %.


Figure 5 LOM micrographs showing the fine scale microstructure in the last bead of the low and high carbon weld metals.

Images taken from the last bead in 7-0.5L200 are presented in Figures 6–7. In agreement with LOM, the former dendritic structure that developed during solidification can be seen. A low magnification overview of the microstructure across a former dendrite is shown in Figure 6. It is seen that the microstructure varies in morphology across the region. When examinations were carried out at high magnifications, it was commonly found that primarily bainite formed in the centre of the dendrites (Figure 7) while a mixture of bainite and a lath-like structure of martensite developed at the prior dendrite boundary regions. In bainitic areas cementite was mainly found at bainitic ferrite boundaries giving upper bainite. A rather large grain is seen in Figure 7 where a group of cementite platelets are penetrating the boundary tip. Cementite of this nature was also observed and characterised elsewhere where coalesced bainite was studied. [12, 16]. Work on weld metals with 7Ni and 2Mn showed that an unusual form of bainite developed.

5
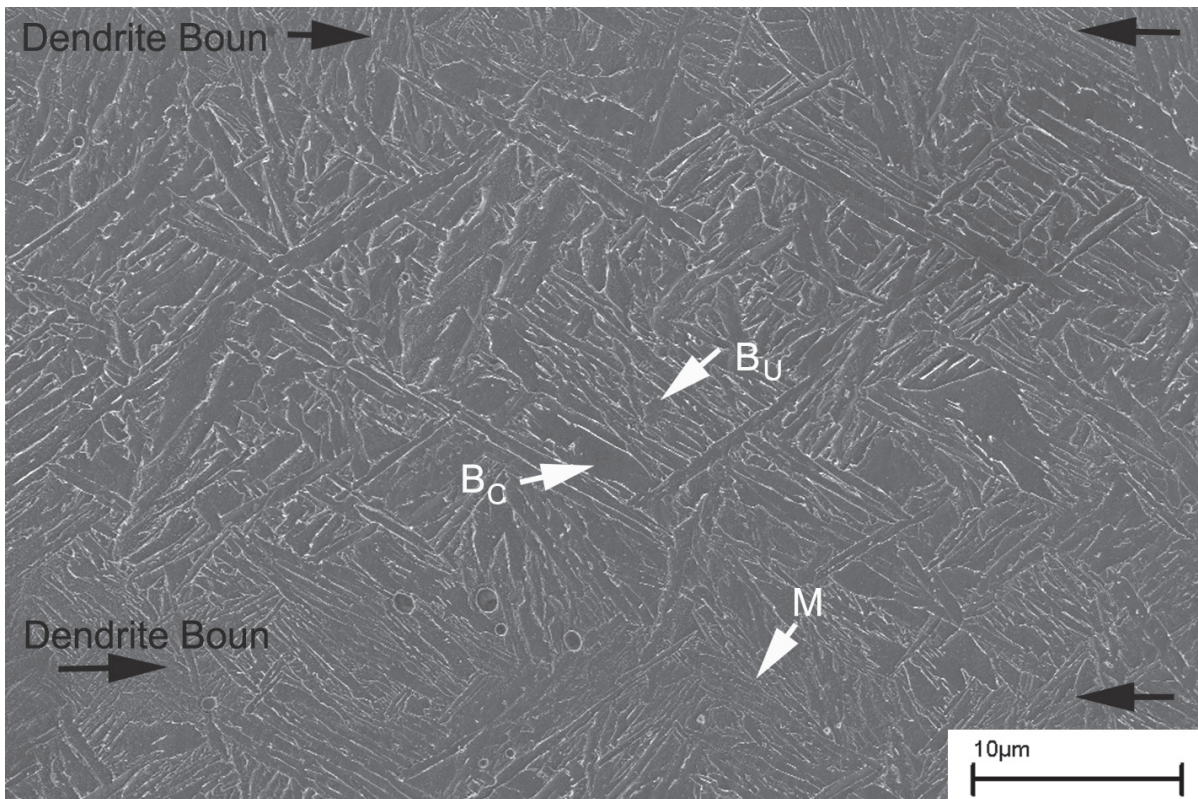
Figure 6 FEGSEM micrograph from 7-0.5L200 of as-deposited weld metal with mainly upper bainite (B_U) and together with coalesced bainite (B_C) found within the former dendrites and predominantly laths of martensite (M) at interdendritic regions.
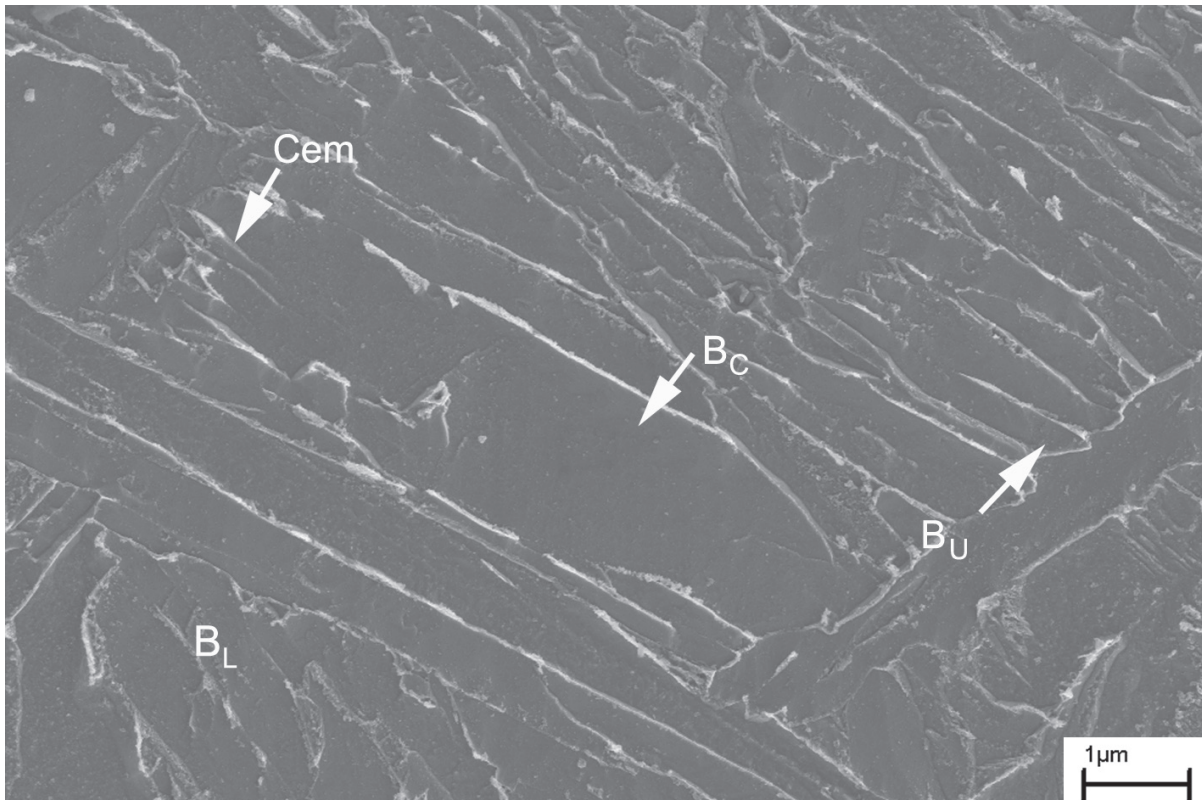
Figure 7 FEGSEM micrograph showing upper bainite (B_U), lower bainite (B_L) and coalesced bainite (B_C) within a former dendrite at higher magnification in as-deposited weld metal of 7-0.5L200.

It had very large bainitic ferrite grains without the typical subunit structure of platelets with cementite at boundaries. However, in the weld metals presented here the size of the coalesced bainite is considerable smaller.

FEGSEM micrographs from the last bead of weld metal 7-0.5H200 are presented in Figures 8 and 9. A very fine scale microstructure was revealed (Figure 8) and when examined at higher magnification found to be a mixture of mainly martensite with some coalesced bainite (Figure 9). Platelets within grains, as seen in Figure 9, were characterised to be cementite using TEM and electron diffraction. Similar cementite platelets were found and identified also in a 7 Ni – 2 Mn low carbon weld metal [12].

Microstructure – Reheated beads
The overall morphology in the centre of a reheated bead in weld metal 7-0.5L200 is shown in Figure 10. In this FEGSEM micrograph it is possible to clearly see the former dendrite boundary regions. The former interdendritic regions show a finer microstructure which is a mixture of tempered martensite and bainite. A comparitively coarse morphology of mainly tempered bainite was found in the dendrite core regions (Figure 11). In both areas cementite precipitates were found at the boundaries and within the bainitic ferrite.

A FEGSEM overview of the centre of a reheated bead in weld metal 7-0.5H200 is shown in Figure 12; the microstructure is generally much finer than in 7-0.5L200 (Figure 10). Overall the microstructure was deemed to be predominantly that of tempered martensite with some tempered bainite. A dendrite core region is shown in Figure 13 where precipitates are found both at the boundaries and within the bainitic ferrite.

Dilatometry
The effect of carbon on the Ac_1 and Ac_3 temperatures was measured using dilatometry. It was found that the Ac_1 and Ac_3 temperatures were at 685 °C and 770 °C respectively for 7-0.5H200 measured at a heating rate of 25 °C / s. These temperatures may be compared to values of 700 °C and 770 °C for Ac_1 and Ac_3 for a low carbon weld metal similar to 7-0.5L200 [10].

Different cooling rates were chosen to characterise the austenite decomposition temperatures in 7-0.5H200. For a cooling rate of 25 °C / s transformation took place at 355 °C and for a very low cooling rate of 1°C / s it was 365 °C. These temperatures may be compared to results with low carbon content (0.03 wt. %) where transformation took place at 490 °C for a cooling rate of approximately 40 °C / s and at 480°C when cooling at 1°C / s.

Discussion

As expected carbon additions proved important not only for the mechanical properties but also for the microstructure in the 7Ni-0.5Mn system. It was found that carbon additions increased
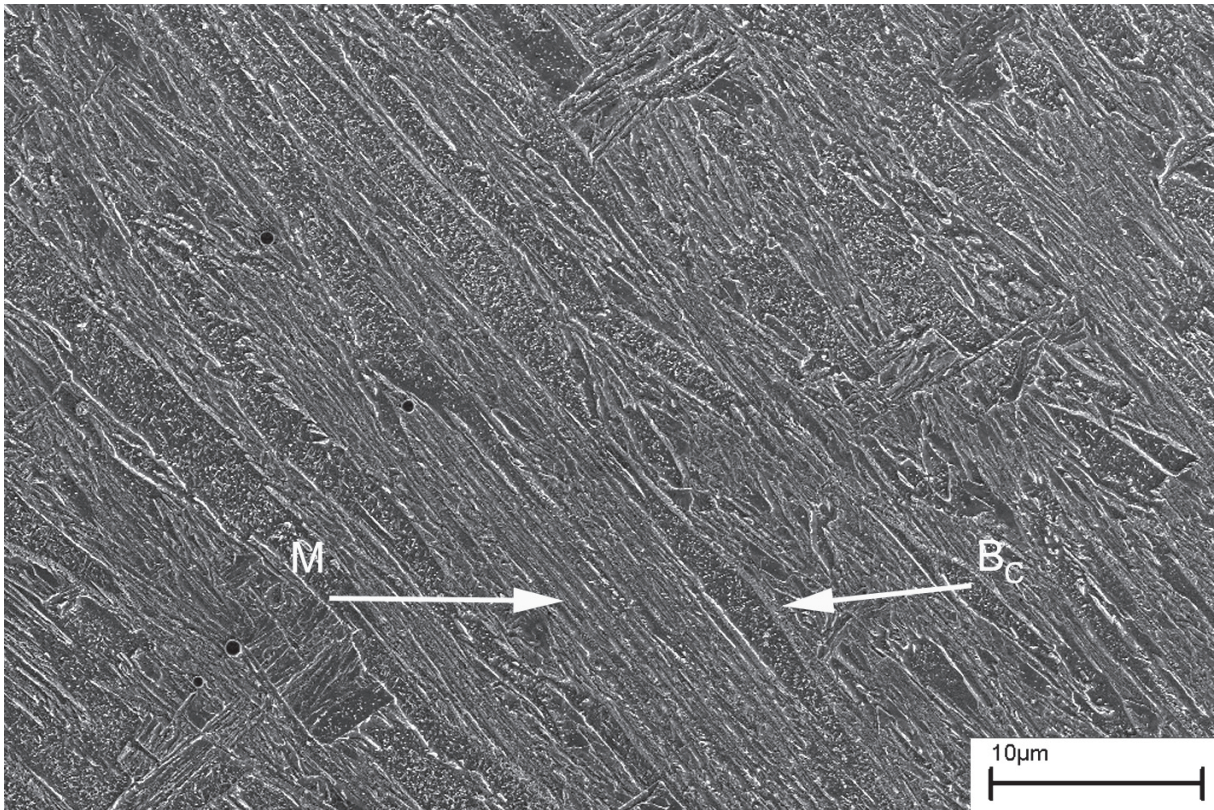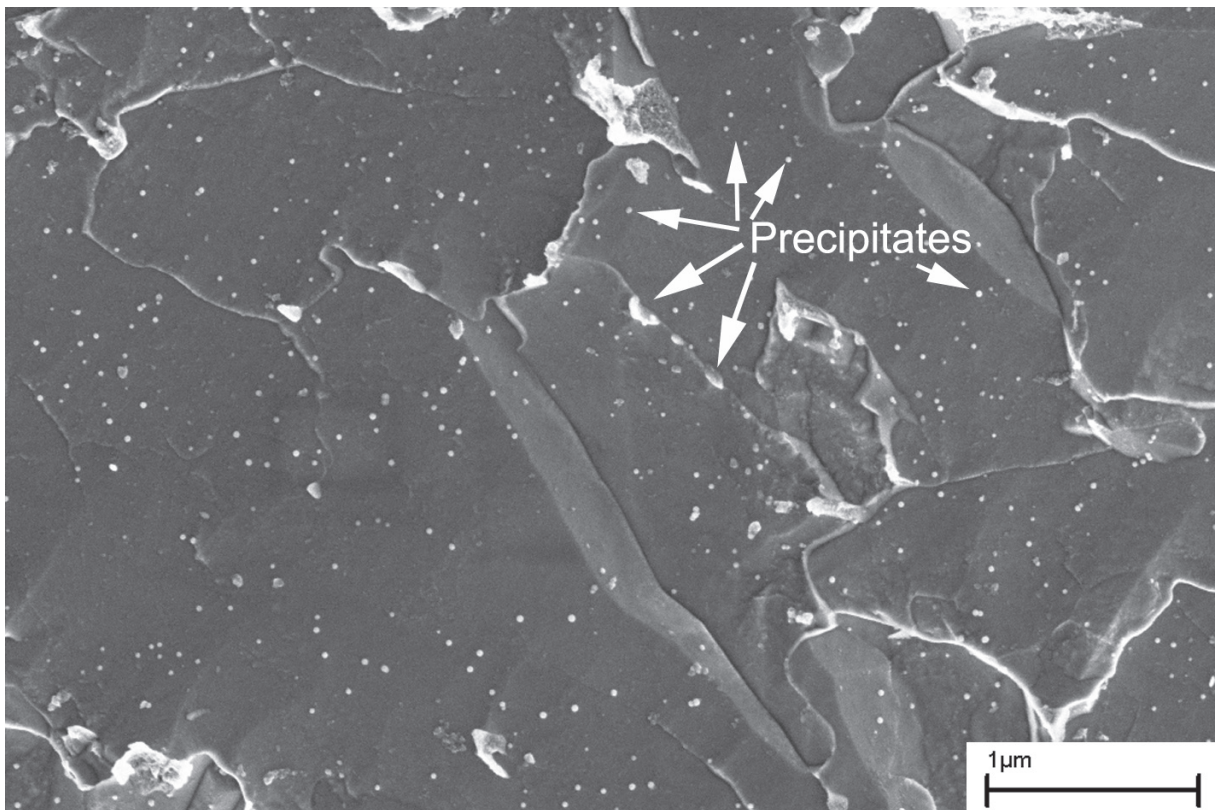
Figure 8 FEGSEM micrograph giving an overview of as-deposited weld metal in 7-0.5H200 where M is martensite and B_C is coalesced bainite.
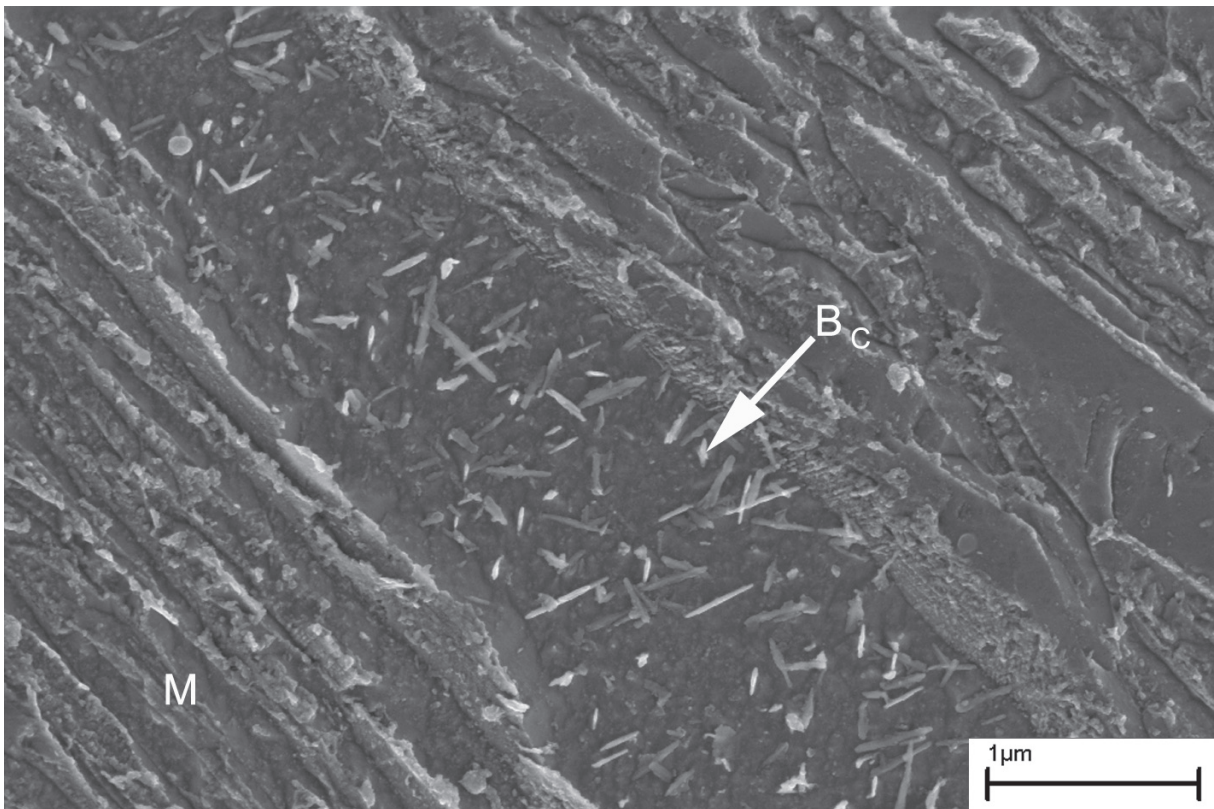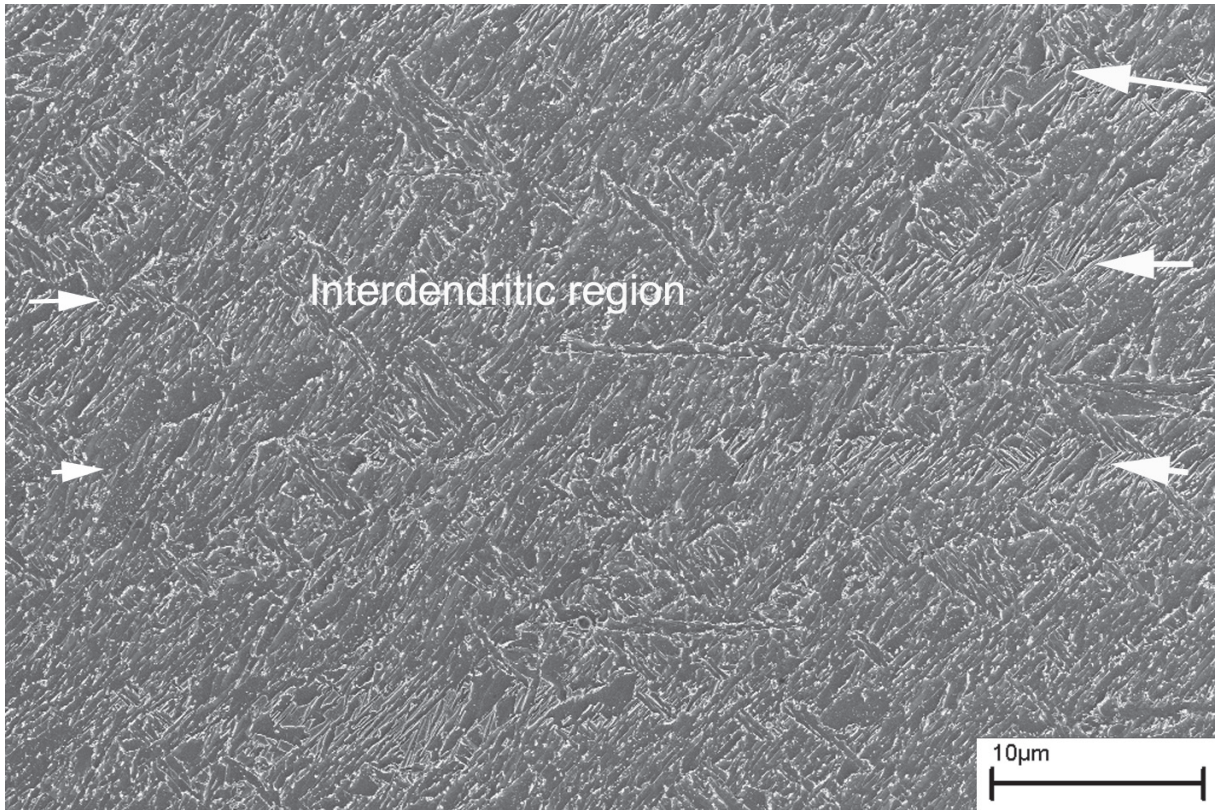

Figure 9 FEGSEM micrograph showing a mixture of coalesced bainite (B_C) and martensite (M) at high magnification in the last bead of weld metal 7-0.5H200.
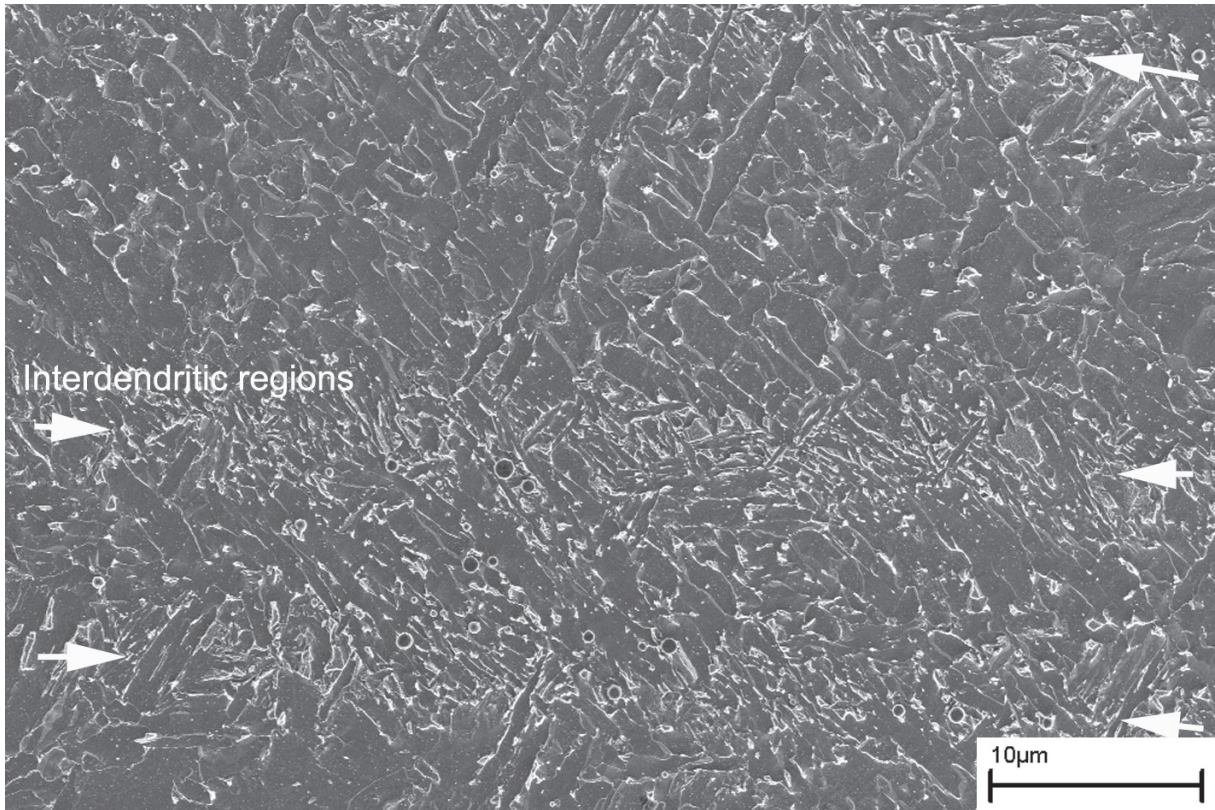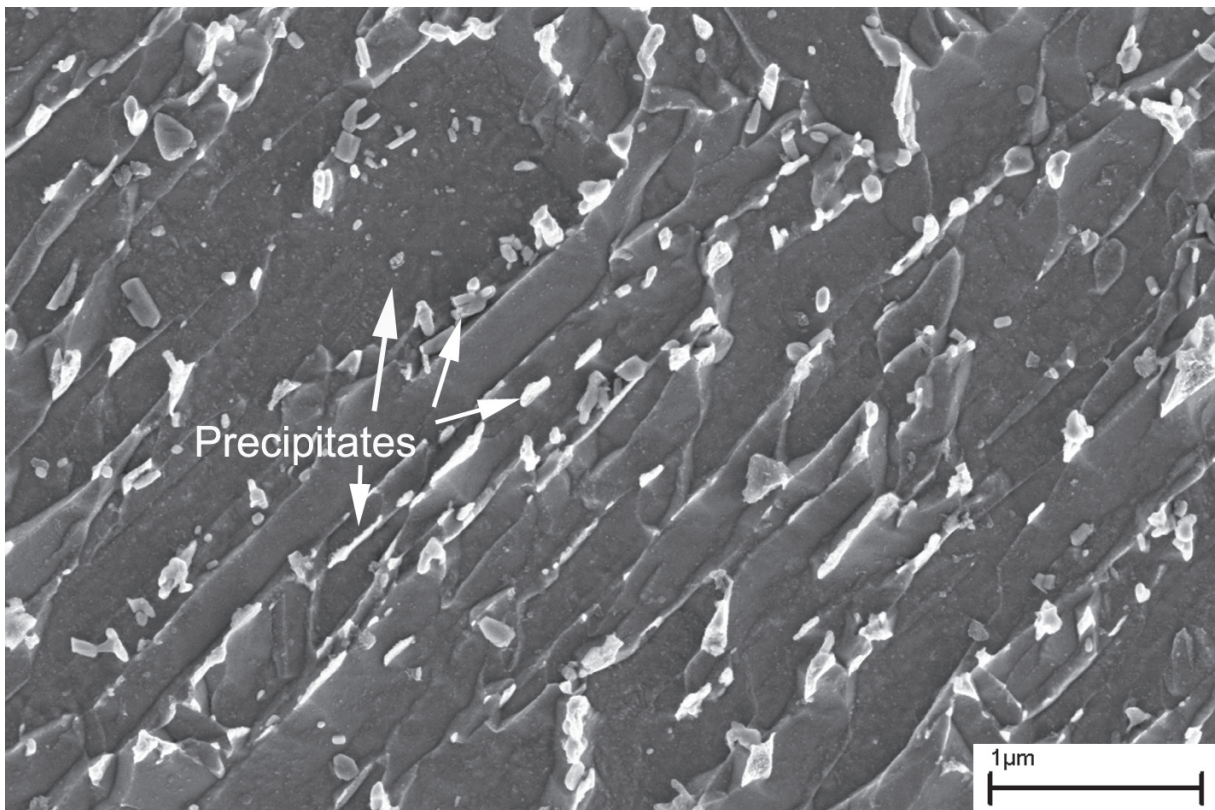
Figure 10 FEGSEM micrograph from weld metal 7-0.5L200 giving an overview in the center of a reheated bead. Here, the former dendrite boundary regions are clearly visible.

Figure 11 FEGSEM micrograph of tempered bainite in the center of a former dendrite in a reheated bead in weld metal 7-0.5L200.

Figure 12 FEGSEM micrograph giving an overview of the microstructure in the center of a reheated bead in weld metal 7-0.5H200.

Figure 13 FEGSEM micrograph showing the center of a dendrite at high magnification in a reheated bead of weld metal 7-0.5H200.

Weld Metal	Main Constituent	Measured transformation temp. / °C	Calculated transformation temp. / °C	
			M_S / °C	B_S / °C
Low Carbon	Bainite	490	395	498
High Carbon	Martensite	355	347	449

Table 2 A comparison between the transformation temperature measured using dilatometry and the transformation temperatures predicted using the empirical equations for B_S and M_S [17-18] for the high and low carbon weld metals.

strength at limited expense to impact toughness. Microstructural investigations revealed a fine scale microstructure with martensite gradually replacing bainite becoming the dominant phase as carbon increased from 0.03 to 0.11 wt. %.

In the low carbon weld metal a mixture of mainly upper bainite along with small amounts of lower and coalesced bainite developed in former dendrite core regions while a fine microstructure of martensitic laths formed at the boundaries (Figure 6). These differences are a consequence of the inevitable chemical segregation associated with the dendritic solidification. The segregation has previously been demonstrated experimentally; nickel and manganese are enriched in the interdendritic regions where a greater quantity of martensite is found [10–11]. Since both elements are austenite stabilisers, it follows that transformation at interdendritic regions takes place at lower temperatures thus promoting martensite.

It was recorded that carbon additions also stabilises austenite to lower transformation temperatures. Transformation with 0.11 wt. % C took place in the region of 355 °C, some 125 °C lower than the 0.03 wt. % C weld metal which transformed around 480 °C. It was decided to estimate the bainite start temperature (B_S) and the martensite start temperature (M_S) temperatures using empirical equations [17–18] for the average composition of the weld metals (Table 1) to allow a comparison with the measured transformation temperatures. With the low carbon weld metal, B_S was estimated to take place at 498 °C while M_S was predicted to be at 395 °C. Repeating the calculation for the high carbon weld metal, a B_S of 449 °C and a M_S of 347 °C were predicted. These predictions are not expected to be accurate since the equations do not extend to the present nickel concentrations. However when calculated and measured transformation temperatures and the observed microstructure are compared, there is surprisingly good agreement (Table 2).

Overall, it is found that increasing the carbon content enhances the formation of martensite and with a level of 0.11wt. %, martensite was not only the dominant phase at the former dendrite boundary regions; but also within the dendrites.

The microstructural changes that took place were reflected in hardness measurements. The decrease in hardness in the 0.03 wt. % C weld metal as reheated regions were encountered may be explained due to redistribution of carbon in the bainitic ferrite platelets along with the coarsening and spheroidising of cementite. In tempered martensitic regions it was also found that precipitation took place with the formation of cementite. The formation of precipitates and the loss of carbon in solid solution results in a large decrease of hardness. As a consequence the largest hardness decrease was observed with the predominantly martensitic high carbon weld metal.

The gradual increase in strength due to carbon additions may be attributed to the fact that the proportion of martensite increases. Martensite gives a smaller effective grain size which is inherited on tempering and contributes to strength and explains the limited loss of impact toughness. The relation between mechanical properties and microstructure is discussed in more detail elsewhere [19].

Conclusions

The influence on structure and properties of carbon additions from 0.03 to 0.11 wt. % were investigated for high strength steel weld metals with 7 Ni and 2 Mn. As predicted by neural network modelling, carbon additions were found positive for strength at minor expense to toughness.

With low carbon content, different types of bainite was characterised using FEGSEM at former dendrite core regions while a lath-like microstructure of martensite was found at interdendritic regions. These differences were attributed to segregation of manganese and nickel. As carbon increased austenite was stabilised to lower transformation temperatures and gradually the microstructure became predominantly martensitic in nature.

Carbon additions were found to promote martensite resulting in a harder and stronger microstructure. The relatively minor reduction in impact toughness as strength increased was attributed to the overall refinement of the microstructure.

Acknowledgements

References
1.   The right welding wire could help the U.S. Navy save millions, Welding Journal, pp. 55 – 58, June 1999.

2. L.-E. Svensson: Svetsaren, 54, January (1999).

3. D.J. Widgery, L. Karlsson, M. Murugananth & E. Keehan, Approaches to the development of high strength weld metals, 2nd Int. Symposium on High Strength Steel, Norway (2002).

4. Y. Kang, H.J. Kim, and S.K. Hwang: ISIJ International (Japan), 40 December (2000), p. 1237.

5. D.J.C. Mackay: Neural Computation. (1992), p. 448.

6. D.J.C. Mackay: Neural Computation. (1992), p. 415.

7. H.K.D.H. Bhadeshia: ISIJ International (Japan), 39, p. 966 October, (1999).

8. M. Murugananth, H. K. D. H. Bhadeshia, E. Keehan, H. O. Andrén, L. Karlsson, Strong and Tough Ferritic Steel Welds, Proc. 6th Int. Seminar, "Numerical Analysis of Weldability", Austria (2001)

9. Zhang Z, Farrar RA, Influence of Mn and Ni on the microstructure and toughness of C–Mn–Ni weld metals, Welding Journal 76 : (5) S183–S196 May1997

10. E. Keehan, L. Karlsson, H.-O. Andrén, H. K. D. H. Bhadeshia, Influence of C, Mn and Ni contents on microstructure and properties of strong steel weld metals, Part II. Impact toughness gain from manganese reductions, In Manuscript.

11. E. Keehan, L. Karlsson, H.-O. Andrén, Influence of C, Mn and Ni contents on microstructure and properties of strong steel weld metals, Part I. Effect of nickel content, In Manuscript

12. E. Keehan, H. K. D. H. Bhadeshia, H.-O. Andrén, L. Karlsson, L.-E. Svensson, Microstructure characterisation of a high strength steel weld metal containing the novel constituent coalesced bainite, In manuscript

13. E. Keehan, M. Murugananth, L. Karlsson, H.-O. Andrén, H. K. D. H. Bhadeshia, New developments with C–Mn–Ni high strength steel weld metals, Part A. Microstructure, In Manuscript

14. SSAB Oxelösund, WeldCalc, Version 1.0.0, 98 – 99.

15. T. Araki, M. Enomoto and K. Shibata: Mater. Trans. JIM, 32 (1991), No. 8. 729

16. H.K.D.H. Bhadeshia, Theory and Significance of Retained Austenite in Steels, Ph.D. thesis, University of Cambridge, 1979

17. R.W.K. Honeycombe & H.K.D.H. Bhadeshia, Steel Microstructure and Properties, 2nd Ed., Edward Arnold, London, 1995, p. 133

18. R.W.K. Honeycombe & H.K.D.H. Bhadeshia, Steel Microstructure and Properties, 2nd Ed., Edward Arnold, London, 1995, p. 103

19. E. Keehan, L. Karlsson, H.-O. Andrén, L.-E. Svensson, New developments with C–Mn–Ni high strength steel weld metals, Part B. Mechanical Properties, In Manuscript